Implementation of the fast charging concept for electric local public transport: the case-study of a minibus

F. Baronti*, R. Di Rienzo*, R. Moras*, R. Roncella*, R. Saletti*, G. Pede§, F. Vellucci§
*Dip. di Ingegneria dell'Informazione - Università di Pisa, Italy
§Laboratorio Veicoli a Basso Impatto Ambientale ENEA Santa Maria di Galeria (Roma), Italy
E-mail: federico.baronti@unipi.it

***Abstract*—This paper shows an effective implementation of the fast charging concept in the electric local public transport context. An electric minibus powered with a lead-acid battery is considered as a case-study. Its traction battery is redesigned using 12 V standard lithium-iron-phosphate modules to benefit from the higher performance of the lithium battery technology compared to the lead-acid one. The minibus can achieve a continuous operation characterised by 20 min of traveling alternated with 10 min of standstill for fast recharging of the battery. Experiments performed on a single module of the battery show that the load profile is sustained without appreciable issues both in temperature and life degradation of the lithium cells.**

I. Introduction

Battery electric vehicles provide an emission-free and quiet way of transport, with lower operation costs than traditional internal combustion engine vehicles. The local public transport systems need to exploit these features, especially inside historical city centres or in restricted areas, such as university campuses and hospitals [1]. As a public bus is expected to operate continuously for many hours a day, providing the required energy in an effective way is a challenging task.

Sizing the onboard traction battery to store all the energy required for one day is indeed impracticable, because of its high cost and weight. Thus, the bus should be supplied with additional energy during service. The time required to reenergise the bus, as well as the infrastructure and operation costs for its implementation, are critical issues.

The depleted battery could be replaced with a charged one (*i.e.*, battery swapping) during the day. This approach is definitely feasible [2], [3] but has the drawback of requiring a special layout of the battery system and a dedicated infrastructure, in order to make the battery swap quick and reliable. The alternative solution is to find a way to recharge the battery during the normal operation of the bus, for instance at dedicated bus stops. The effectiveness of this approach is strictly connected to the capability of fast recharging, so that the bus can be reenergised without significantly reducing the useful operation time or availability of the vehicle.

It is worth noting that the a-priori knowledge of the bus routes and driving profiles can be used advantageously to optimise the design of the battery and the recharging policy. Given this premise, some studies based on simulations have shown the feasibility of the fast recharging concept for fostering the electrification of local public transport [4]–[6]. This work aims at taking a further step towards the implementation of the fast recharging concept for a small electric bus, suitable for operation in historical centres and restricted areas.

In order to keep the initial cost for the implementation of the fast recharging system as low as possible, commercial-off-the-shelf (COTS) components and already available solutions are preferred to custom ones. This might lead to a non optimal implementation, but with affordable initial costs, a target hardly achievable with a custom design approach. First of all, we considered an electric minibus powered by lead-acid batteries, as the vehicle to be adapted to experiment the fast recharging concept. This implies that the battery has to be redesigned completely, by employing the lithium-ion chemistry, which is much more appropriate for fast charging. To this end, standard 12 V lithium-iron-phosphate (LFP) [7] battery modules, already developed for another application [8], are used. A battery charger selected from commercial products completes the case-study considered in this work.

After a detailed description of the three case-study elements in Section II, the system-level design of the minibus with fast recharge will be given in Section III. Some preliminary experimental results are shown in Section IV and some conclusions are drawn at the end of the manuscript.

II. Case-study

A. Electric minibus

The main characteristics of the electric minibus considered in this work are reported in Table I. The bus was originally equipped with a 72 V 585 A h lead-acid battery, organised in two modules placed in the rear of the vehicle and weighing around 1200 kg. The traction battery has to be redesigned using LFP cells, which have higher performance than lead-acid ones, with the constraint of fitting the new cells in the same volume as the original lead-acid battery.

B. Standard 12 V battery module

As mentioned above, the redesign of the traction battery is based on the reuse of standard parts or components already developed for other applications enjoying the benefit of reduced costs. The new battery is thus built with standard 12 V LFP battery modules [8]. This choice facilitates the

TABLE I
CHARACTERISTICS OF THE CASE-STUDY ELECTRIC MINIBUS

Curb weight (without the traction battery)	4800 kg
Original lead acid battery voltage and capacity	72 V and 585 A h
Volume available for the traction battery	2x $(1210 \times 541 \times 375)\,\mathrm{mm}^3$
Length	5.1 m
Traction power/torque	25 kW/235 N m
# Passengers	30 (10 of which are seated)
Average energy consumption per kilometer	$500\,\mathrm{W\,h\,km}^{-1}$

(a) (b)

Fig. 1. (a) Photograph of the 30 A h, 60 A h and 100 A h module prototypes (from right to left); (b) 3D view of the new version of the 60 A h module.

replacement of the original lead-acid battery, as the required battery voltage can be obtained by connecting six modules in series. Furthermore, the use of standard modules minimises the battery cost, because of the high production volumes expected for a standard 12 V LFP battery module. In fact, the latter finds application in many fields, especially for the replacement of the traditional lead-acid automotive battery for starting-lighting-ignition functions. The standard module consists of four series-connected LFP cells and an advanced BMS. The module is available with three different capacities, *i.e.*, 30 A h, 60 A h and 100 A h. The main electrical and mechanical characteristics of the three modules are reported in Table II. Figure 1 shows a prototype of the three modules with different capacities.

1) Advanced BMS: The developed standard module is provided with advanced monitoring and management functions, which are essential for an effective use of lithium-ion batteries. These functions are implemented by the Module Management Unit (MMU), which is connected to the 4 LFP cells of the module. A simplified block diagram of the MMU is shown in Fig. 2 The core of the MMU is a 32-bit ARM Cortex-M3 microcontroller, which manages the acquisition of the voltage and temperature of the 4 cells (via a dedicated stack monitor IC), the activation of the module fans (which are controlled so that the maximum cell temperature is kept between two configurable thresholds) and the communication with other modules and subsystems building up the battery via

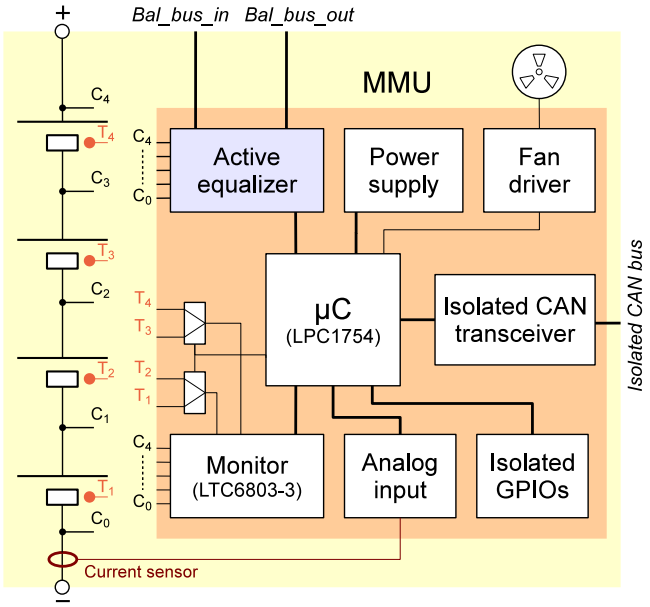

Fig. 2. Schematic block diagram of the Module Management Unit (MMU). C_4-C_0 and T_4-T_1 labels indicate, respectively, the connections from the cells' terminals and temperature sensors to the MMU electronics.

an isolated Controller Area Network (CAN) bus. The MMU also incorporates a section for handling analog inputs and isolated general purpose (GP) I/Os. One of the analog input channel can be used to acquire the module current. If modules are series-connected to form a battery string, the current sensor will be connected to just one module, which will share this information to the other modules via the CAN bus. The module current is numerically integrated by the microcontroller as part of the State-of-Charge (SoC) estimation algorithm [9], which is based on the Coulomb Counting method combined with Open Circuit Voltage (OCV) compensation. The isolated GPIOs can be used to control the protection switch of the battery string.

An innovative function of the MMU is the circuit for active charge equalisation. It is based on an isolated DC/DC converter and a switch matrix, which allows the individual connection of each module cell to the converter output (its input is connected to the module's terminals), thus implementing a module to cell active balancing topology [10]. A novel and interesting feature of the circuit is the possibility of connecting the converter output also to a cell in another module, thus making it possible to achieve inter-module active balancing. This is obtained by a circular balancing bus (*Bal_bus_in* and *Bal_bus_out* signals in Fig. 2), handled in a way so that the battery is never short circuited, independently of any decision taken by the single microcontrollers in the MMUs [11].

C. Battery charger

A fundamental element for the continuous operation of the electric minibus is the battery charger, which should enable the fast recharging of the battery during the bus stops. Bearing in mind the reduction of the initial cost, the battery charger was

TABLE II
CHARACTERISTICS OF THE 12 V LFP MODULES

Nominal voltage V	12.8	12.8	12.8
Capacity (A h)	30	60	100
Volume (mm^3)	277 × 160 × 208	262 × 159 × 283	310 × 186 × 318
Weight (kg)	8.3	10.3	19.1
Max charging current (A)	60	120	200
Max discharging current (A)	90	180	300

(a) (b)

Fig. 3. (a) Charger module; (b) Assembled 4 charger modules.

TABLE III
CHARACTERISTICS OF THE BATTERY CHARGER

Input	400 V three-phase AC , 50–60 Hz
Output voltage	60–87.6 V
Continuous output current	360 A
Continuous power @ 72.8 V	26 kW
Efficiency	>85 %

selected from the commercial available devices. In more detail, the selected charger consists of four identical modules (Mod. RG9, manufactured by Zivan s.r.l, www.zivan.it) connected in parallel and assembled, as shown in Fig. 3. The main characteristics of the charger are reported in Table III.

III. SYSTEM DESIGN

This section discusses the system design of the electric minibus, in order to achieve a continuous operation with fast recharging. The first step is the redesigning of the traction battery using the 12 V LFP battery modules.

A. Battery redesign

The minibus traction battery is redesigned to obtain the same nominal terminal voltage of the original lead-acid battery. The value of 72 V is easily achieved by series-connecting six standard modules to form a *string*, as shown in Fig. 4. To complete the sizing of the battery, we have to select the module capacity (among the 30 A h, 60 A h and 100 A h values) and the number n of parallel-connected strings, bearing in mind the geometrical constraints on the battery size (see Table I). In fact, the maximum value of n is determined by the bottom surface of the two housings available for the battery. The possible values of n are reported in Table IV, together with the main features of the resulting traction battery.

Table IV suggests that the 60 A h standard module is the most appropriate choice for building up the traction battery.

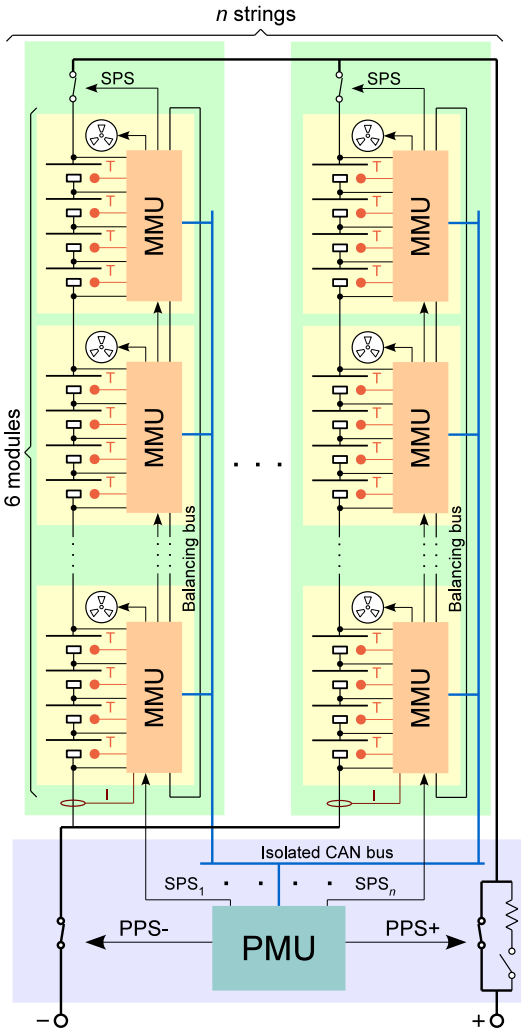

Fig. 4. Architecture of the redesigned traction battery including the Battery Management System.

TABLE IV
MAIN FEATURES OF THE TRACTION BATTERY BUILT UP WITH THE THREE STANDARD MODULES

Module capacity (A h)	30	60	100
Number of strings n	4	4	3
Battery capacity (A h)	120	240	300
Stored energy (kW h)	9.2	18.4	23.0
Cont. discharging power (kW)	27.6	55.3	69.1
Cont. charging power (kW)	18.4	36.9	46.1
Battery weight (kg)	199	295	344
Area occupation (%)	81	90	79

Indeed, 24 60 A h modules can be placed into the 2 housings, arranged in $n = 4$ parallel-connected strings. This sizing allows the full exploitation of the recharging power provided by the selected charger (*i.e.*, 26 kW), which is a key aspect for a fast recharging scenario and cannot be achieved using the 30 A h module that can sustain up to 18.4 kW. Moreover, the battery configuration using the 60 A h modules is easier to assemble (as two strings can be allocated in each frame) lighter and cheaper than the one based on the 100 A h modules. The latter provides more energy and power, but the power requirements imposed by the case-study electric minibus and charger are already fully met by the 60 A h modules.

To complete the redesign of the battery, we need to provide the battery with a BMS. This can easily be achieved by the cooperation of the MMUs present in the standard modules, which communicate via the CAN bus, and the supervision of the Pack Management Unit (PMU). The latter provides the battery interface towards the other subsystems of the minibus and the off-board charger and controls the pack protection and pre-charge switches (PPS+ and PPS-), as well as the string protection switches (SPSs). As visible in Fig. 4, the *Bal_bus_in* and *Bal_bus_out* signals of the 6 MMUs in each of the 4 strings are connected to create the Balancing bus used for inter-module active charge equalisation.

B. Minibus operation mode

It is now possible to assess the achieved operation mode of the designed minibus with fast recharge. First of all, we observe that the driving range with the fully charged battery is around 37 km, which roughly corresponds to 1.8 h of travelling time, assuming an average speed of 20.8 km h^{-1}. This provides a good flexibility in setting the operation mode of the bus. To this end, we assume that the battery charger is available at a single bus stop (*e.g.,* the terminal bus stop), in order to reduce the installation costs. To assess the performance, we compute the charging time per one hour of operation, which yields the balance between the energy consumed during the travelling time and the recharged energy [4].

Let us define C the average energy consumption per kilometre, P_{chg} the available charging power, T_{run} the travelling time, $T_{\mathrm{chg}}^{'}$ the net charging time, T_{off} the overhead of the charging time due to the connection and disconnection of the minibus to the battery charger, $T_{\mathrm{chg}} = T_{\mathrm{chg}}^{'} + T_{\mathrm{off}}$ the total charging time, $T_{\mathrm{op}} = T_{\mathrm{run}} + T_{\mathrm{chg}}$ the minibus operation time, and v the average speed of the minibus (which accounts for the short stops during the bus route). To guarantee a net balance between the energy flowing in and out the battery, the ratio r of $T_{\mathrm{chg}}^{'}$ to T_{run} must fulfil the following equation

$$r = \frac{T_{\mathrm{chg}}^{'}}{T_{\mathrm{run}}} = \frac{Cv}{P_{\mathrm{chg}}} = 0.4, \qquad (1)$$

where $C = 500\,\mathrm{W\,h\,km^{-1}}$, $v = 20.8\,\mathrm{km\,h^{-1}}$, and $P_{\mathrm{chg}} = 26\,\mathrm{kW}$ in our case-study.

To calculate the overall charging time per one hour of operation, we also need to consider T_{off}, which is proportional to the number of recharges in one hour. Assuming that the minibus is performing two complete routes in one hour (and thus two recharges) and that 1 min is the time needed for the manual plugging or unplugging of the charger connector, we end up to $T_{\mathrm{off}} = 4\,\mathrm{min}$. This yields to an overall charging time per one hour of operation ($T_{\mathrm{op}} = 1\,\mathrm{h}$) of

$$T_{\mathrm{chg}} = T_{\mathrm{chg}}^{'} + T_{\mathrm{off}} = \frac{rT_{\mathrm{op}} + T_{\mathrm{off}}}{1 + r} \approx 20\,\mathrm{min} \qquad (2)$$

This means that the basic route of the bus consists approximately of 20 min of travelling time and 10 min of standstill time at the recharging bus stop. Even if the 33 % achieved ratio of the charging time to the operation time is not outstanding [4], it can be considered a valuable result as the major design focus was to keep the initial costs for the implementation of the fast recharging concept as low as possible. Moreover, T_{off} can reasonably be shortened by an automatic mechanism to connect the battery's terminals to the charger (*e.g.*, a pantograph or a robotised arm, or wireless power transfer), with benefits also in terms of operation of the minibus, but at the expense of higher initial costs. We finally observe that the SoC swing during the route is around 20 % and the battery energy is fully restored to the initial level after recharge. This rather small SoC swing does not stress the battery and helps in extending its life. Moreover, it also gives the flexibility to shorten the length of the terminal bus stops during rush hours, by accepting only a partial refill of the battery energy. The battery could then be brought back to the optimal SoC starting value by increasing the bus stop length during off-peak hours.

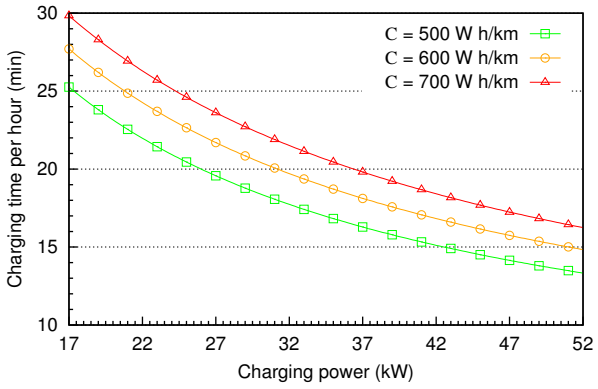

Fig. 5. Overall charging time per one hour of operation, as a function of the available recharging power. Three different energy consumptions of the minibus per kilometre are shown.

In order to investigate the possible system performance improvement that comes from a different level of the available charging power, Fig. 5 shows the charging time per one hour of operation, as a function of the available charging power. The figure also shows the dependence on the average energy consumption per kilometre of the minibus. Assuming that the battery charger could provide the maximum continuous charging power allowed for the selected LFP cells of 36.9 kW, the charging time could be shortened to 16 min every hour. Given the available charging power of 26 kW, the charging

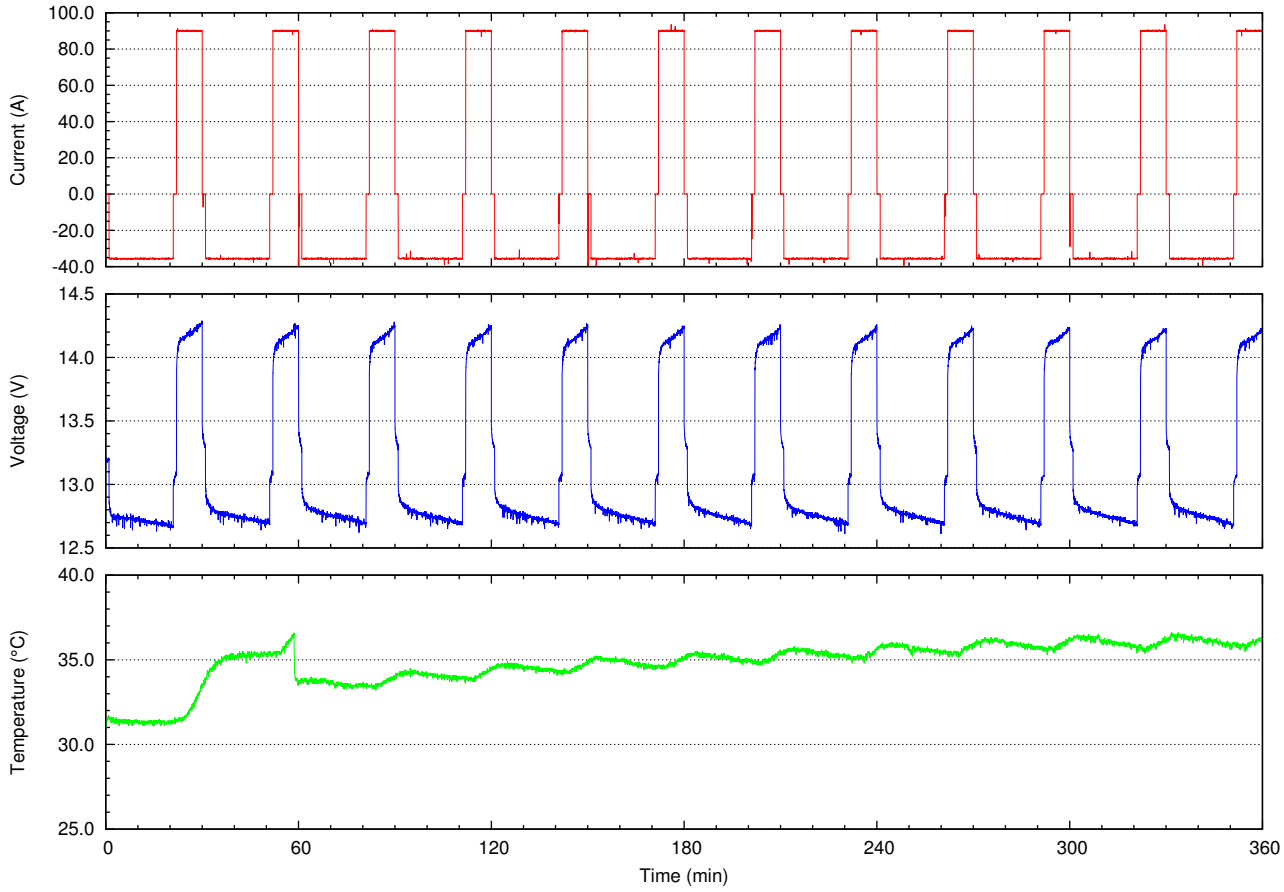

Fig. 6. Behaviour of the module current, voltage, and temperature during the 6 h test.

time increases to 22 min and 24 min, if the average energy consumption of the minibus is 600 W h km^{-1} and 700 W h km^{-1}, respectively.

IV. Experimental results

Even if the ultimate goal is to validate the design with the implementation of a complete system (including the electric minibus with the redesigned battery and recharging station), a fundamental preliminary step is the assessment of the 60 A h 12 V standard module to withstand the current profile determined by the operation mode of the minibus derived in the previous section. To this end, a module is being tested with a periodic stepwise current profile lasting 30 min and thus simulating a complete bus route. The profile consists of the following steps:

- 1 min of zero current. This step accounts for the time passing from the end of the recharge phase to the minibus leaving the bus stop;
- 20 min of −35.7 A. This step simulates the average power that the battery supplies to the minibus during traveling. The module current is determined considering that each of the four battery strings has the nominal voltage of 72.8 V and delivers one forth of the average traction power of 10.4 kW.
- 1 min zero current. This step accounts for the time from the minibus stopping at the bus stop to the beginning of the recharge phase;
- 8 min of 89.3 A. This step simulates the fast recharge phase of the battery. The module current is determined considering that each of the four battery strings has the nominal voltage of 72.8 V and receives one forth of the charging power of 26 kW.

The tests are performed on a 60 A h module by connecting the cells to a battery tester (which generates the above described current profile) and the module BMS to a PC via the CAN bus. In this way, the PC can log the voltage and temperature of the four cells, which are acquired by the BMS and sent as CAN message data. The complete test consists of 12 repetitions of the current profile and lasts 6 h. The test is started after a full charge of the battery and carried out at the room temperature of around 26 °C. Thus, the SoC is going to swing in the 80 %–100 % range. The module current, voltage, and temperature acquired during the test are shown in the Fig. 6.

It is worth noting that no appreciable temperature increase is observed during the first discharge phase, while the module temperature grows during the fast recharge step, as it might be expected. After around 1 h, the module temperature reaches 36.5 °C a value at which the module fans are activated. As they

remain active until the temperature decreases below 32 °C, it is worth noting how the temperature rise during the fast recharge is much less than before and the module reaches a rather stationary temperature condition at the end of the test. This is an encouraging result showing that the operation profile with frequent and fast recharging of the battery is not going to create thermal issues.

Another important point is the effect of the current profile on the ageing of the battery. This assessment requires long tests, which are still running. However, by extrapolating data from life tests carried out on a single cell with the same chemistry as the one used in the standard module, we foresee that the redesigned battery can provide more than 4800 h of bus operation (equivalent to 100 000 km) before the residual capacity reaches 80 % of the initial value [12].

Currently, the 24 modules are going to be assembled into the two housings fitting into the available space in the rear part of the minibus. A 3D model of the battery is shown in Fig. 7, where a half of each container allocates 6 modules belonging to the same string. In the figure, the PMU with signal and power connectors towards the 4 strings and the extern of the battery are also recognisable. The wiring harness for the signal and power connection of the modules in a string and to the PMU is omitted for the sake of simplicity. The overall battery weight is approximately 450 kg, which is a remarkable result as the original lead-acid battery weighed 1200 kg.

Fig. 7. 3D view of the redesigned battery of the minibus. Wiring harness is not shown.

V. Conclusions

This paper has described the implementation of the fast charging concept in the framework of local electric public transport. The major driving force in the design choices was to keep the initial costs of the system as low as possible. To this end, a conventional electric minibus, a commercial battery charger and standard 12 V LFP modules, developed in previous studies, were considered as a starting point. This work has shown the redesign of the minibus battery, which was originally based on lead-acid cells, using the standard modules and discussed a possible operation mode of the bus that keeps the battery SoC in a 20 % range during the operation time. This is achieved by alternating 20 min of travelling with 10 min of charging. Thus, the duty cycle of useful operation of the minibus is 66 %. This can be considered a good result as it has been obtained trying to minimise the initial costs of the system, which can be estimated approximately in € 20 000, of which € 5000 for the battery charger, € 12 000 for the battery and the remainder for ancillary components, assembly and installation costs. Preliminary results have shown that the designed battery can withstand the charging and load profile of the application. Currently, the battery is being assembled and installed on the vehicle for laboratory and on the road tests.

References

[1] X. C. Wang and J. A. González, "Assessing Feasibility of Electric Buses in Small and Medium-Sized Communities," *International Journal of Sustainable Transportation*, vol. 7, no. 6, pp. 431–448, Nov. 2013.

[2] W. Choi and J. Kim, "Electrification of public transportation: Battery swappable smart electric bus with battery swapping station," in *2014 IEEE Conference and Expo Transportation Electrification Asia-Pacific (ITEC Asia-Pacific)*. IEEE, Aug. 2014, pp. 1–8.

[3] M. R. Sarker, H. Pandzic, and M. A. Ortega-Vazquez, "Optimal Operation and Services Scheduling for an Electric Vehicle Battery Swapping Station," *IEEE Transactions on Power Systems*, vol. 30, no. 2, pp. 901–910, Mar. 2015.

[4] P. Sinhuber, W. Rohlfs, and D. U. Sauer, "Conceptional considerations for electrification of public city buses - Energy storage system and charging stations," in *2010 Emobility - Electrical Power Train*. IEEE, Nov. 2010, pp. 1–5.

[5] ——, "Study on power and energy demand for sizing the energy storage systems for electrified local public transport buses," in *2012 IEEE Vehicle Power and Propulsion Conference*. IEEE, Oct. 2012, pp. 315–320.

[6] L. Buzzoni and G. Pede, "New prospects for public transport electrification," in *2012 Electrical Systems for Aircraft, Railway and Ship Propulsion*. IEEE, Oct. 2012, pp. 1–5.

[7] M. S. Whittingham, "History, Evolution, and Future Status of Energy Storage," *Proceedings of the IEEE*, vol. 100, no. Special Centennial Issue, pp. 1518–1534, May 2012.

[8] F. Baronti, G. Fantechi, R. Roncella, R. Saletti, G. Pede, and F. Vellucci, "Design of the battery management system of LiFePO4 batteries for electric off-road vehicles," in *2013 IEEE International Symposium on Industrial Electronics*. IEEE, May 2013, pp. 1–6.

[9] Y.-M. Jeong, Y.-K. Cho, J.-H. Ahn, S.-H. Ryu, and B.-K. Lee, "Enhanced Coulomb counting method with adaptive SOC reset time for estimating OCV," in *2014 IEEE Energy Conversion Congress and Exposition (ECCE)*. IEEE, Sep. 2014, pp. 1313–1318.

[10] J. Gallardo-Lozano, E. Romero-Cadaval, M. I. Milanes-Montero, and M. A. Guerrero-Martinez, "Battery equalization active methods," *Journal of Power Sources*, vol. 246, pp. 934–949, Jan. 2014.

[11] F. Baronti, C. Bernardeschi, L. Cassano, A. Domenici, R. Roncella, and R. Saletti, "Design and Safety Verification of a Distributed Charge Equalizer for Modular Li-Ion Batteries," *IEEE Transactions on Industrial Informatics*, vol. 10, no. 2, pp. 1003–1011, May 2014.

[12] F. Baronti, R. Roncella, R. Saletti, G. Pede, and F. Vellucci, "Smart LiFePO4 battery modules in a fast charge application for local public transportation," in *AEIT Annual Conference - From Research to Industry: The Need for a More Effective Technology Transfer (AEIT), 2014*, Sep. 2014, pp. 1–6.